New evidence for deformation in ^{73}Zn

M. Huhta,[1] P.F. Mantica,[1,2] D.W. Anthony,[1,2] P.A. Lofy,[1,2] J.I. Prisciandaro,[1,2]

R.M. Ronningen,[1] M. Steiner,[1] and W.B. Walters[3]

[1] *National Superconducting Cyclotron Laboratory, Michigan State University, East Lansing, Michigan 48824*

[2] *Department of Chemistry, Michigan State University, East Lansing, Michigan 48824*

[3] *Department of Chemistry and Biochemistry, University of Maryland, College Park, Maryland 20742*

(July 29, 1998)

Abstract

The beta decay of ^{73}Cu to levels in ^{73}Zn has been studied. The ^{73}Cu nuclides were produced by fragmentation of ^{76}Ge projectiles having energies of 70 MeV/nucleon in a 202 mg/cm^2 thick ^{9}Be target. Beta and γ singles, β-γ and γ-γ coincidence data were collected and used to construct the low-energy level scheme of ^{73}Zn. New spin-parity assignments have been deduced for some excited states in ^{73}Zn based on measured β decay branching ratios and systematics of other $N = 43$ isotones. A 195-keV transition was identified in ^{73}Zn with a half-life of 13.0(2) ms, a value several orders of magnitude shorter than previously reported, and is consistent with an $M2$ multipolarity. The low-energy level structure of ^{73}Zn is shown to be consistent with particle-triaxial rotor model calculations employing a ground state quadrupole deformation with $\beta_2 = 0.2$.

I. INTRODUCTION

The experimental study of β unstable nuclei in the region $Z \approx 28$, $N > 40$ is important for the testing and further development of theoretical models to better describe the properties of exotic neutron-rich nuclei important to the astrophysical r-process and the progression of shell structure towards the neutron drip-line. These nuclei have proven difficult to study due to low production rates. Runte *et al.* [1,2] completed decay studies of the neutron-rich Cu isotopes using multinucleon transfer reactions and on-line isotope separation. Two-proton pickup reactions [3] have been used to obtain spectroscopic information for low-energy states in the Zn isotopes through $A = 74$. Fission also provides a means to access this region of the chart of the nuclides. Winger *et al.* [4,5] utilized thermal neutron induced fission of ^{235}U to obtain detailed spectroscopic information on the low energy states of even-even Zn isotopes populated following the β decay of odd-odd Cu isotopes up to $A = 76$. Recently, relativistic fission has been employed [6] to produce new neutron-rich nuclei in the region $28 < Z < 44$ including the doubly-magic nucleus ^{78}Ni [7].

Projectile fragmentation has also proven to be a powerful method for the production of medium-mass, neutron-rich nuclei. For example, the production and half-life determination of heavy Ni isotopes up to ^{76}Ni has been accomplished by fragmentation of ^{86}Kr [8]. The recent improvements in the intensity of metal primary beams at the National Superconducting Cyclotron Laboratory at Michigan State University has allowed access to regions of the chart of the nuclides previously unavailable for nuclear structure measurements. A metal beam of particular interest for the study of neutron-rich nuclides in the region $Z > 28$ is ^{76}Ge. By fragmenting a 70 MeV/nucleon ^{76}Ge beam in a Be target, we were able to produce secondary beams of several $A \approx 70$ nuclides with sufficient intensities to perform β-γ and γ-γ spectroscopic studies on these species. The observed production rate of 80 ^{73}Cu nuclei per second per 5 pnA primary ^{76}Ge beam was nearly an order of magnitude larger than the ^{73}Cu production rate measured for proton-induced superasymmetric fission of ^{238}U coupled with IGISOL [9]. Thus, experimental production rates of secondary fragments produced fol-

lowing the interaction of an intermediate energy heavy-ion beam and a low Z target compare favorably with rates obtained in fission experiments.

In this paper, we report on the low-energy level structure of ^{73}Zn populated following the β decay of ^{73}Cu. With only 5 particles outside the $Z = 28$, $N = 40$ semi-magic shell closure, one would expect this nuclide to exhibit modest collective features. However, a transition from spherical to deformed structure was observed [10] in both the Ge and Ga isotopes with the addition of two neutrons, from $N = 40$ to 42. The low energy levels of ^{73,74}Zn determined from the two-proton pickup experiments by Bernas *et al.* [3] and the systematics of the 2_1^+ states in the even-even Zn isotopes hint at a similar transition in these nuclides. The Hartree-Fock-Bogoliubov (HFB) calculations in Ref. [3] predict small oblate deformation ($\beta_2 = -0.1$) for ^{71}Zn but a much larger prolate deformation ($\beta_2 = +0.2$) for ^{73}Zn. This would suggest that the $N = 40$ subshell is weakened within close approach to the $Z = 28$ proton shell closure.

II. EXPERIMENTAL TECHNIQUE

The measurements were completed using the K1200 Cyclotron and the A1200 fragment separator at the National Superconducting Cyclotron Laboratory at Michigan State University. Radioactive nuclei were produced by fragmentation of ^{76}Ge^{+19} projectiles having energies of 70 MeV/nucleon in a 202 mg/cm^2 thick ^{9}Be target. The A1200 fragment separator [11] with a 70 mg/cm^2 Al wedge at its second dispersive image was used to separate the fragments. The momentum acceptance was set to 1% of the central Bρ using a slit at the first momentum dispersed image of the A1200. Further M/q separation was achieved using the Reaction Product Mass Separator (RPMS). Identification of secondary fragments at both the A1200 focal plane and the experimental endstation was accomplished by measuring the fragment energy loss in 300 μm Si PIN detectors and the fragment time-of-flight (TOF) between a thin plastic detector at the first dispersive image of the A1200 and the PIN detectors. The A1200 was tuned to the peak of the momentum yield curve for ^{73}Cu

secondary fragments. Other activities identified by ΔE-TOF at the RPMS tail for this setting of the A1200 included ^{70,71}Ni, ^{72}Cu and ^{74,75}Zn.

The desired ^{73}Cu beam was implanted into a collection wheel consisting of nine aluminium collection foils equally spaced around the circumference. Movement of the wheel was achieved using a stepper motor, whose controller was interfaced to the data acquisition system. A complete counting cycle consisted of a beam implantation period, a decay period, and a wheel movement period. Data acquisition was enabled during both the implantation and decay periods. Both data acquisition and beam implantation were blocked during each wheel movement, which took approximately 250 ms. The counting cycle intervals were optimized for the particular species under study. For the ^{73}Cu β decay measurements, implantation and decay times of 6 s and 12 s, respectively, were chosen.

The collection wheel was placed at 45-deg to the beam axis to optimize the placement of β and γ-ray detectors around the implantation position. Two 3 mm thin plastic scintillators coupled to photomultiplier tubes were used for detecting β-particles. Two Ge detectors with efficiencies of 80% and 120% at 1.33 MeV relative to a 3"x 3" NaI detector were used to detect γ radiations. The energy resolutions of the 80% and 120% detectors were 2.9 keV and 2.2 keV, respectively, using the 1.33 MeV transition in ^{60}Co. The β and γ-ray detectors were arranged as scintillator-Ge pairs in close geometry on both sides of the implantation point of the collection wheel, with the plastic beta detectors placed immediately in front of the Ge detectors. One scintillator-Ge pair was located directly behind the collection foil. The second scintillator-Ge pair was placed at a 90-deg angle with respect to the beam direction, approximately 40 mm from the point of implantation. The total β efficiency of the plastic scintillators in the selected geometry was measured to be 40(2)%. Experimental β and γ ray singles and β-γ and γ-γ coincidence data were collected event-by-event and written to 8 mm magnetic tape.

III. RESULTS AND DISCUSSION

A part of the β-gated γ-spectrum is shown in Fig. 1. Isotope identification in this spectrum was based on the known γ-ray transitions and half-lives deduced from our multiscaled γ ray data. Transitions belonging to the β decay of ^{73}Cu were first identified by Runte *et al.* [1] at 199, 307, 450, 502, and 674 keV, and a half-life of 3.9(3) s was determined for ^{73}Cu from the decay characteristics of the 450-keV transition. The decay curves for transitions assigned to the β-decay of ^{73}Cu and the 228-keV transition from the β decay of ^{75}Zn, the most abundant contaminant mass, are shown in Fig. 2. A weighted mean of the measured half-lives for the five transitions shown in Fig. 2 results in a value of 4.4(3) s for the half-life of ^{73}Cu, which is consistent with the previously measured value of 3.9(3) s [1].

The proposed level scheme for ^{73}Zn shown in Fig. 3 is based on γ-γ coincidence data, intensity balances, and sum-energy considerations. The γ-γ coincidence spectra for the 674-keV and 1559-keV transitions in ^{73}Zn are shown in Fig. 4 and both are observed to be coincident with the 450-keV transition. The logft values were determined for the decay of ^{73}Cu using intensity balance information and a Q_β- value of 6.25 MeV [12]. A ground-state β branch of 42(12)% was deduced from the difference between the total number of β particles, determined from the growth curve of 218-keV transition associated with ^{73}Ga, and β feeding to excited states.

Systematics of the neutron-rich odd-A Cu isotopes suggest spin and parity $I^\pi = 3/2^-$ for the ground state of ^{73}Cu. The ground state spin and parity of ^{73}Zn is most likely $I^\pi = 1/2^-$ (see, for example, Ref. [3]). This assignment is supported by the fact that the β decay of the ground state of ^{73}Zn to the $5/2^-$ state in ^{73}Ga has a logft value greater than 7.

A strong β branch is observed to the 450 keV state in ^{73}Zn, which deexcites via γ emission only to the ground state. The logft value of 5.2 to this state suggests an allowed β transition and we have tentatively assigned $I^\pi = 3/2^-$ to this state. The levels at 307, 502, 1124, and 2009 keV are all fed weakly in β decay and the deduced logft values of ≈ 6 suggest that these are all negative parity states with spin values of 1/2, 3/2, or 5/2.

The collection of γ-ray singles data during the growth and decay periods made it possible to detect short-living (millisecond) isomers. With the A1200 tuned to the peak production of ^{73}Zn, we identified a short-lived 195-keV transition in the γ ray singles spectrum, whose decay curve is shown in Fig. 5. These data were obtained using a 30 ms growth period and a 100 ms decay period, and the deduced half-life of 13.0(2) ms is several orders of magnitude faster than the $T_{1/2} = 5.8(8)$ s 195-keV isomeric transition assigned to ^{73}Zn by Runte *et al.* [2]. Our new measured half-life for the 195-keV transition in ^{73}Zn restricts the multipolarity of this transition to $M2$, when using the Weisskopf estimates, which establishes the spin and parity of the 195-keV state in ^{73}Zn to be $I^{\pi} = 5/2^{+}$.

No evidence was found in our β-γ coincidence data for the presence of a 199-keV transition having $T_{1/2} \approx 3.9$ s as reported in Ref. [1] (see Fig. 1). Also, all transitions below 100 keV were too low in energy to penetrate the endcaps of our p-type Ge detectors. Therefore we could neither confirm nor refute the existence of a $T_{1/2} = 5.8$ s isomeric transition at 42 keV as reported by Runte *et al.* [2]. Such an isomeric transition would be reasonable to consider in ^{73}Zn, where a low-energy $9/2^{+}$ level may be present a few tens of keV above the $5/2^{+}$ isomeric state. The expected $E2$ transition rate between such closely-positioned states would be slow.

The proposed level scheme for ^{73}Zn in Fig. 3 agrees well with the level information obtained for ^{73}Zn using the two-proton one-neutron pickup reaction (^{14}C,^{17}O) on a ^{76}Ge target by Bernas *et al.* [3]. They identified levels at 280(40), 500(40), and 1140(40) keV, which correspond to the 307, 502, and 1124 keV levels identified in this work. To interpret the level structure of ^{73}Zn, Bernas *et al.* employed HFB calculations to obtain potential energy curves for both ^{71}Zn and ^{73}Zn. While the ground state shape of ^{71}Zn was suggested to be slightly oblate ($\beta_2 \approx -0.1$), a shape change to a more deformed prolate structure was proposed for ^{73}Zn. At $\beta_2 = +0.2$ the HFB calculations predict low-energy states in ^{73}Zn having $J^{\pi} = 1/2^{-}$, $5/2^{+}$, $5/2^{-}$, and $3/2^{+}$. Such a transition to a more deformed shape was also observed between ^{73}Ge and ^{75}Ge [10].

Paar has explained the ordering of positive parity states in the $N = 43$ isotones using

the cluster approach [13]. In his description the low-energy positive-parity states of ^{75}Ge are a consequence of the competition between the $(g_{9/2})^3$, $(g_{9/2})^2(d_{5/2})$ and $(g_{9/2})^2(g_{7/2})$ configurations. The $I^\pi = 7/2^+$ state is the lowest energy positive parity state in ^{75}Ge and can be attributed to the appearance of a $6-j$ symbol in the recouplings for a $g_{9/2}$-hole cluster configuration which is only positive for $J = 7/2$. The lowering of the $I^\pi = 5/2^+$ state to be the lowest energy positive parity state in ^{73}Zn is due to a stronger particle-field coupling strength, i.e. stronger collectivity of quadrupole vibrations in this nuclide [14]. The $5/2^+$ ground state of ^{75}Se has been attributed to a large particle quadrupole-phonon interaction strength [15].

We have performed particle-triaxial rotor model (PTRM) calculations [16,17] in an attempt to reproduce the low-energy level structure of $^{73}Zn_{43}$ and $^{75}Ge_{43}$. The similarities of the low-energy structures of these isotones is evident in Fig. 6, where the systematics of the low-energy positive parity states in the odd-mass $N = 43$ nuclides from ^{73}Zn through ^{79}Kr are given. Although ^{73}Zn lies only two protons off the $Z = 28$ shell closure and the microscopic-macroscopic calculations of Möller *et al.* [18] predict an ϵ_2 value of only 0.06, results of other global calculations, for instance the Extended Thomas-Fermi Strutinsky Integral (ETFSI) approach [19] predict moderate prolate ground state deformation ($\beta_2 = 0.24$) for ^{73}Zn and ^{75}Ge. Our new measurement offers an opportunity to explore which prediction is more accurate in this region of the chart of the nuclides.

The PTRM calculations involved the diagonalization of the deformed shell-model hamiltonian to compute single-particle energies and wave functions of a nonaxially symmetric deformed Woods-Saxon potential [20,21]. The quadrupole deformation parameters were initially taken from Ref. [19], and β_4 and γ were both taken as zero. Positive and negative parity states were calculated separately (no octupole deformation) considering all Nilsson orbitals within ± 7 MeV of the Fermi surface. The relative positions of the positive parity states to the negative parity states were determined from available experimental data. The residual pairing interaction was treated within the BCS approximation, where a standard value of the pairing strength parameter G was adopted for each isotope using the prescription

given in Ref. [22]. The core 2^+ energies were taken from the neighboring even-even nuclides. The recoil terms in the hamiltonian were treated as one-body operators. Attenuation of the Coriolis matrix elements by a factor 0.7 was used to reduce the mixing between intrinsic states and to lower the energy of non-spin aligned members of the band build upon the intruder $\nu\,[422]\,5/2^+$ orbital. A similar attenuation factor was used by Meyer *et al.* [23] to reproduce the properties of the ground state band built on the $\pi\,[422]\,5/2^+$ orbital observed in ^{99}Y.

The results of the PTRM calculations for ^{75}Ge and ^{73}Zn are shown in Figs. 7 and 8, respectively. The final β_2 values were very close to those predicted by the ETFSI calculation [19]. The density of negative and positive parity states below 1 MeV and the ordering of the $7/2^+$, $5/2^+$, and $9/2^+$ triplet of states below 200 keV in ^{75}Ge is reproduced by the PTRM calculations using a prolate ground state deformation of $\beta_2 = 0.22$. The multipole mixing ratio $\delta(E2/M1)$ for the $9/2_1^+ \rightarrow 7/2_1^+$ transition in ^{75}Ge, experimentally determined as -0.11, was calculated to be $\delta(E2/M1) = -0.05$ using the above parameters. However, the predicted half-life of 1.4 ns for the $5/2_1^+$ state is shorter than the measured value of 216 ns, and the mostly $E2$ character of the $5/2_1^+ \rightarrow 7/2_1^+$ is not reproduced. The predicted magnetic dipole moment for the $I = 1/2^-$ ground state in ^{75}Ge of $+0.46\ \mu_N$ is near to the measured value of $+0.51\ \mu_N$ [24]. The branching ratios for γ-ray transitions between low-energy states in ^{75}Ge are compared with calculated values in Table II.

The one feature of the low-energy structure of ^{75}Ge that is absent from the PTRM calculations is the $1/2^-$ state at 885-keV. The first excited $1/2^-$ state is predicted to reside at 2.85 MeV with the parameter set outline above. Small changes in β_2 and the core 2^+ energy did not significantly improve this deficiency in the calculations. We therefore looked systematically at the effects on the calculated structure of ^{75}Ge considering a non-symmetric core deformation. The energy spectrum and transition probabilities for the negative parity states in ^{75}Ge were calculated including triaxial core deformations in the range $15° < \gamma < 55°$. For these PTRM calculations, β_2, β_4 were fixed to 0.22 and 0, respectively, and all other parameters were unchanged. The γ dependence of the negative parity energy spectrum of

^{75}Ge is shown in Fig. 9. The calculated position of the $1/2_2^-$ state moves from 2.5 MeV at $\gamma = 15°$ to a mimimum energy of 740 keV at $\gamma = 30°$. The other dramatic effect is the change in the spacing between the $3/2^-$ and $5/2^-$ members of the $\nu\,[301]\,1/2^-$ ground state band. The triaxial deformation value expected for ^{75}Ge can be estimated in the rigid triaxial rotor model. Using the energy of the 2_1^+ and 2_2^+ states in the even-even neighbors ^{74}Ge and ^{76}Ge [26], γ values of 29° and 30° are extracted for these two isotopes, respectively. The predicted γ-ray branching ratios for a core deformation $\beta_2 = 0.22$, $\gamma = 30°$, $\beta_4 = 0$ are compared to experimental values and the PTRM results obtained when $\gamma = 0°$ in Table II. The low-energy negative parity levels in ^{75}Ge are better reproduced by considering non-symmetric core rotation; however, there was better agreement between the experimental branching ratios and the PTRM calculations when $\gamma = 0°$ was used.

Although only limited experimental information is available for ^{73}Zn, the results of the PTRM calculations (Fig. 8) are encouraging. The calculations using a ground state quadrupole deformation of $\beta_2 = 0.20$ predict the lowest positive parity state to be $5/2^+$, with a wavefunction that is highly mixed between the $\nu\,[422]\,5/2^+$, $\nu\,[431]\,3/2^+$, and $\nu\,[440]\,1/2^+$ deformed single-particle states. Two other positive parity states having I^π=$7/2^+$, $9/2^+$ are also predicted at low energy, where the $9/2^+$ state may be responsible for the $T_{1/2} = 5.8$ s isomeric state in ^{73}Zn identified by Runte *et al.* [2]. The next set of positive parity levels are predicted to lie around 1 MeV. The experimental states observed in ^{73}Zn fed in the β decay of ^{73}Cu are most likely negative parity states, and map well with those calculated within the PTRM. The lowest negative parity state is predicted to be $1/2^-$ and is predominately $\nu\,[301]\,1/2$. The first excited state is the bandhead of the $\nu\,[303]\,5/2$ deformed single particle orbital. Both the $3/2_1^-$ and $5/2_2^-$ states are members of the ground state band and are predicted to decay primarily to the $1/2^-$ ground state, as is observed experimentally (see Fig. 3). The $3/2_1^- \rightarrow 1/2_1^-$ transition is calculated to be mostly $M1$ ($\delta(E2/M1) = +0.245$) and the theoretical $B(E2; 5/2_2^- \rightarrow 1/2_1^-)$ value of 0.029 e^{2}b^2 is at least three times larger than that calculated for the other transitions depopulating the $5/2_2^-$ state.

In summary, we have studied the β decay of ^{73}Cu to gain information on the low-energy

level structure of ^{73}Zn. A 195-keV $M2$ isomeric transition in ^{73}Zn has been identified which connects the $5/2^+$ lowest energy positive parity state to the $1/2^-$ ground state of ^{73}Zn. Using the particle-triaxial rotor model, we have demonstrated that the low-energy states in ^{73}Zn are consistent with a nucleus having moderate quadrupole deformation ($\beta_2 \approx 0.2$), consistent with the global ETFSI calculations. This moderate quadrupole deformation in the ground state of ^{73}Zn suggests a weakening of the $N = 40$ subshell in close vicinity to the $Z = 28$ proton shell closure. In examining the low-energy structure of the $N = 43$ isotone ^{75}Ge, triaxiality may prove important in the description of negative parity states in this region above the $Z = 28$ proton closed shell.

IV. ACKNOWLEDGMENTS

This work has been supported by the National Science Foundation under Contract No. PHY-9528844. The authors thank the operations staff of the NSCL for the successful completion of these measurements, J.A. Winger for his design of the collection wheel apparatus, and R. Harkewicz and the ECR group at the NSCL for development of the ^{76}Ge beam. The guidance provided by P.B. Semmes in use of the PTRM computer codes is also gratefully acknowledged.

REFERENCES

[1] E. Runte, W.-D. Schmidt-Ott, P. Tidemand-Petersson, R. Kirchner, O. Klepper, W. Kurcewicz, E. Roeckl, N. Kafrell, P. Peuser, M. Bernas, P. Dessagne, M. Langevin, and K. Rykaczewski, Nucl. Phys. **A399**, 163 (1983).

[2] E. Runte, K.-L. Gippert, W.-D. Schmidt-Ott, P. Tidemand-Petersson, L. Ziegeler, R. Kirchner, O. Klepper, P. O. Larsson, E. Roeckl, D. Schardt, N. Kafrell, P. Peuser, M. Bernas, P. Dessagne, M. Langevin, and K. Rykaczewski, Nucl. Phys. **A441**, 237 (1985).

[3] M. Bernas, P. Dessagne, M. Langevin, J. Payet, F. Pougheon, P. Roussel, W.-D. Schmidt-Ott, P. Tidemand-Petersson, and M. Girod, Nucl. Phys. **A413**, 363 (1984).

[4] J.A. Winger, John C. Hill, F.K. Wohn, E.K. Warburton, R.L. Gill, A. Piotrowski, and D.S. Brenner, Phys. Rev. C **39**, 1976 (1989).

[5] J.A. Winger, John C. Hill, F.K. Wohn, E.K. Warburton, R.L. Gill, A. Piotrowski, R.B. Schuhmann, and D.S. Brenner, Phys. Rev. C **42**, 954 (1990).

[6] P. Armbruster, M. Bernas, S. Czajkowski, H. Geissel, T. Aumann, Ph. Dessage, C. Donzaud, E. Hanelt, A. Heinz, M. Hesse, C. Kozhuharov, Ch. Miehe, G. Munzenberg, M. Pfutzner, K.-H. Schmidt, W. Schwab, C. Stephan, K. Summerer, L. Tassan-Got, and B. Voss, Z. Phys. **A355**, 191 (1996).

[7] C. Engelmann, F. Ameil, P. Armbruster, M. Bernas, S. Czajkowski, Ph. Dessage, C. Donzaud, H. Geissel, A. Heinz, Z. Janas, C. Kozhuharov, Ch. Miehe, G. Munzenberg, M. Pfutzner, C. Rohl, W. Schwab, C. Stephan, K. Summerer, L. Tassan-Got, and B. Voss, Z. Phys. **A352**, 351 (1995).

[8] F. Amiel, M.Bernas, P. Armbruster, S. Czajkowski, Ph. Dessagne, H. Geissel, E. Hanelt, C. Kozhuharov, C. Hiehe, C. Donzaud, A. Grewe, A. Heinz, Z. Janas, M. de Jong, W. Schwab, and S. Steinhäuser, Eur. Phys. J. A **1**, 275 (1998).

[9] M. Huhta, P. Dendooven, A. Honkanen, A. Jokinen, G. Lhersonneau, M. Oinonen, H. Penttilä, K. Peräjärvi, V. A. Rubchenya and J. Äystö, Phys. Lett. **B405**, 230 (1997)

[10] M.N. Vergnes, G. Rotbard, F. Guilbaut, D. Ardouin, C. Lebrun, E.R. Flynn, D.L. Hanson, and S.D. Orbesen, Phys. Lett. **72B**, 447 (1978).

[11] B.M. Sherrill, D.J. Morrissey, J.A. Nolen, Jr., and J.A. Wigner, Nucl. Instr. Methods **B56/57**, 1106 (1991)

[12] G. Audi, O. Bersillon, J. Blachot and A. H. Wapstra, Nucl. Phys. **A624**, 1 (1997)

[13] V. Paar, Nucl. Phys. **A211**, 29 (1973)

[14] L.S. Kisslinger, Nucl. Phys. **78**, 341 (1966).

[15] Y. Tokunaga, H. Seyfarth, O.W.B. Schult, S. Brant, V. Paar, D. Vratner, H.G. Börner, G. Barreau, H. Faust, Ch. Hofmyer, K. Schreckenbach, and R.A. Meyer, Nucl. Phys. **A430**, 269 (1984).

[16] S.E. Larsson, G.A. Leander, and I. Ragnarsson, Nucl. Phys. **A307**, 189 (1978).

[17] I. Ragnarsson and P.B. Semmes, Hyperfine Interactions **43**, 425 (1988).

[18] P. Möller, J.R. Nix, W.D. Myers, and W.J. Swiatecki, At. Data Nucl. Data Tables **59**, 185 (1995).

[19] Y. Aboussir, J.M. Pearson, A.K. Dutta, and F. Tondeur, At. Data Nucl. Data Tables **61**, 127 (1995).

[20] W. Nazarewicz, J. Dudek, R. Bengtsson, T. Bengtsson, and I. Ragnarsson, Nucl. Phys. **A435**, 397 (1985).

[21] S. Cwiok, J. Dudek, W. Nazarewicz, J. Skalski, and T. Werner, Comput. Phys. Commun. **46**, 379 (1987).

[22] J. Dudek, A. Majhofer, and J. Skalski, J. Phys. G **6**, 447 (1980).

[23] R.A. Meyer, E. Monnard, J.A. Pinston, F. Schussler, I. Ragnarsson, B. Pfeiffer, H. Lawin, G. Lhersonneau, T. Seo, and K. Sistemich, Nucl. Phys. **A439**, 510 (1995).

[24] A.F. Oluwole, S.G. Schmelling, and H.A. Shugart, Phys. Rev. C **2**, 228 (1970).

[25] Y. Ishikawa, N. Kato, S. Suematsu, and T. Kuroyanagi, Nucl. Phys. **A403**, 396 (1983)

[26] *Table of Isotopes, 8th Edition*, R.B. Firestone and V.S. Shirley, eds. (Wiley, New York, 1996).

FIGURES

FIG. 1. Part of the β-gated γ-spectrum of ^{73}Cu. Isotope identification was based on β decay half-lives, known γ-ray energies, and ΔE-TOF information prior to implantation. The γ ray transitions assigned to ^{73}Cu are indicated. Unlabelled transitions can be attributed to the β decay of: ^{70}Cu, ^{71,74,75}Zn, and ^{73,74,75}Ga.

FIG. 2. Decay curves for proposed β-delayed γ ray transitions from ^{73}Cu. A representative curve for the 228-keV β-delayed γ ray transition from ^{75}Zn, the major isotopic contaminant, is also shown.

FIG. 3. Proposed decay scheme for ^{73}Zn populated via the β decay of ^{73}Cu. The logft values are deduced using a Q_β value of 6.25 MeV [12].

FIG. 4. Gamma-ray coincidence spectra for the 674-keV and 1559-keV transitions assigned to ^{73}Zn. The 450-keV transition is observed in both coincidence gates.

FIG. 5. Portions of the γ ray singles and β-γ coincidence spectra collected during implantation when the A1200 was tuned for peak production of ^{73}Zn. The growth and decay curve for the 195-keV isomeric transition assigned to ^{73}Zn is shown in the inset.

FIG. 6. Systematics of the low-energy positive parity states in the $N = 43$ isotones.

FIG. 7. Experimental levels in ^{75}Ge compared to those resulting from the PTRM calculations discussed in the text.

FIG. 8. Experimental levels in ^{73}Zn compared to those resulting from the PTRM calculations discussed in the text.

FIG. 9. Variation in the calculated negative parity energy spectrum for ^{75}Ge as a function of the triaxial deformation parameter γ. The calculations assume a fixed quadrupole deformation of $\beta_2 = 0.22$ and $\beta_4 = 0$. The observed negative parity states below 1.5 MeV in ^{75}Ge are also shown.

TABLES

TABLE I. Energies, relative intensities and observed coincidences for γ-rays following the β decay of ^{73}Cu. The energy values have an error of ± 0.2 keV, while the error in the deduced γ-ray intensity is given in parentheses.

E_γ(keV)	E_{level}(keV)	I_{rel}	Coincident γ-lines
195.5	195.5	—	—
307.2	307.2	12(1)	—
449.6	449.6	100(4)	674,1559
502.2	502.2	17(2)	—
674.4	1124.0	7(1)	450
1559.3	2008.9	2(1)	450

TABLE II. Experimental branching ratios for ^{75}Ge compared to results of PTRM calculations for an axially symmetric rotor ($\beta_2 = 0.22$, $\gamma = 0°$) and a triaxial rotor ($\beta_2 = 0.22$, $\gamma = 30°$).

			Experimental	PTRM Results	
I_i	I_f	E_γ(keV)	Branching	$\gamma = 0°$	$\gamma = 30°$
$5/2_2^-$	$5/2_1^-$	140	—	0.5	13
$5/2_2^-$	$3/2_1^-$	204	99	98	29
$5/2_2^-$	$1/2_1^-$	457	100	100	100
$3/2_2^-$	$5/2_2^-$	118	—	0.2	50
$3/2_2^-$	$5/2_1^-$	258	1	0.1	223
$3/2_2^-$	$3/2_1^-$	322	5	20	1147
$3/2_2^-$	$1/2_1^-$	575	100	100	100
$7/2_1^-$	$3/2_2^-$	76	—	—	—
$7/2_1^-$	$5/2_2^-$	194	—	5	27
$7/2_1^-$	$5/2_1^-$	334	—	100	100
$7/2_1^-$	$3/2_1^-$	398	—	—	2
$1/2_2^-$	$3/2_2^-$	310	60	41	24
$1/2_2^-$	$5/2_2^-$	428	10	—	2
$1/2_2^-$	$5/2_1^-$	568	13	—	19
$1/2_2^-$	$3/2_1^-$	632	42	86	1180
$1/2_2^-$	$1/2_1^-$	885	100	100	100
$\mu(1/2_1^-)$			$+0.51\ \mu_N$	$+0.46\ \mu_N$	$+0.45\ \mu_N$

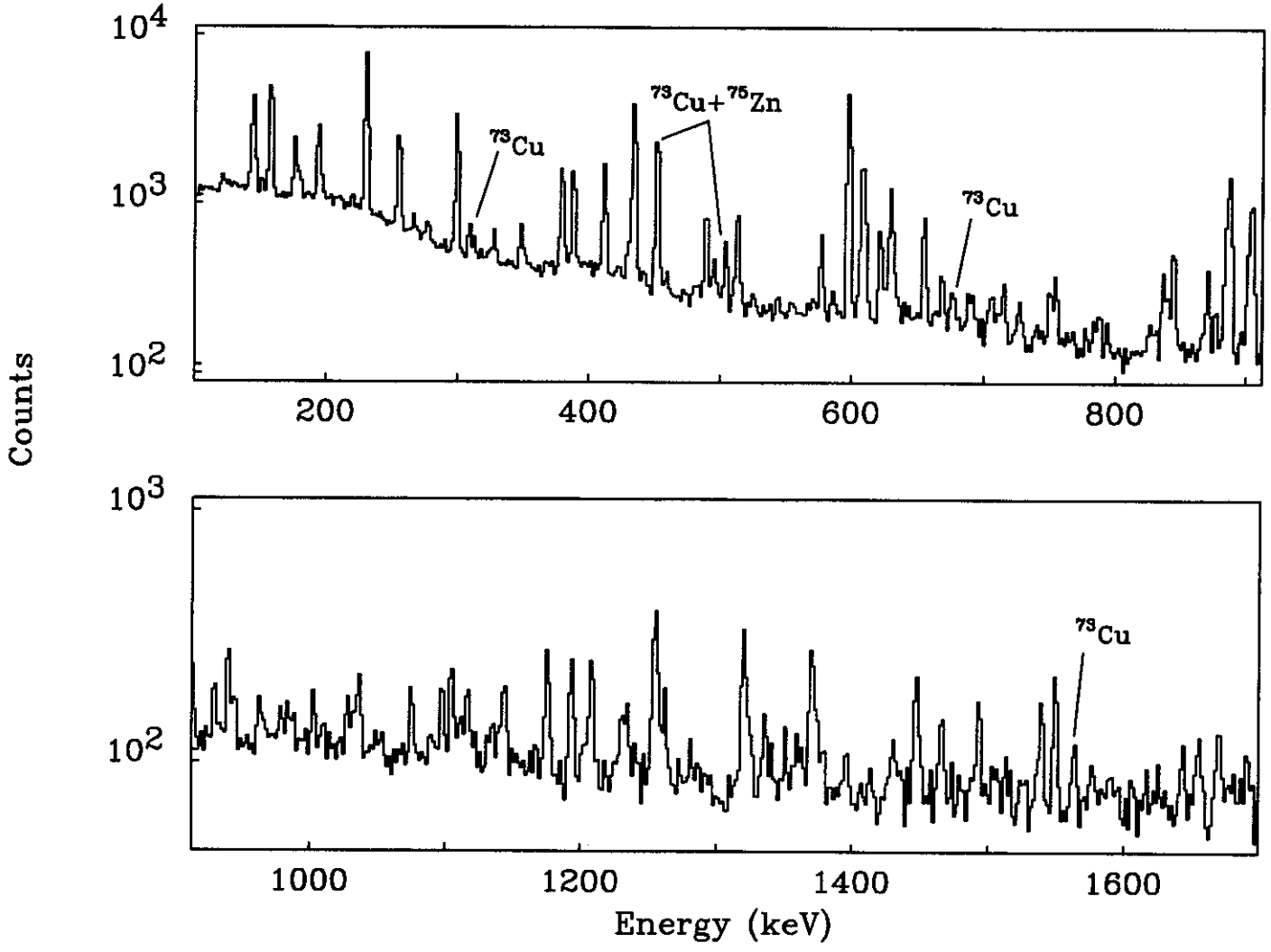
Counts
10^4
10^3
10^2
^{73}Cu
^{73}Cu+^{75}Zn
^{73}Cu
200
400
600
800
10^3
10^2
^{73}Cu
1000
1200
1400
1600
Energy (keV)

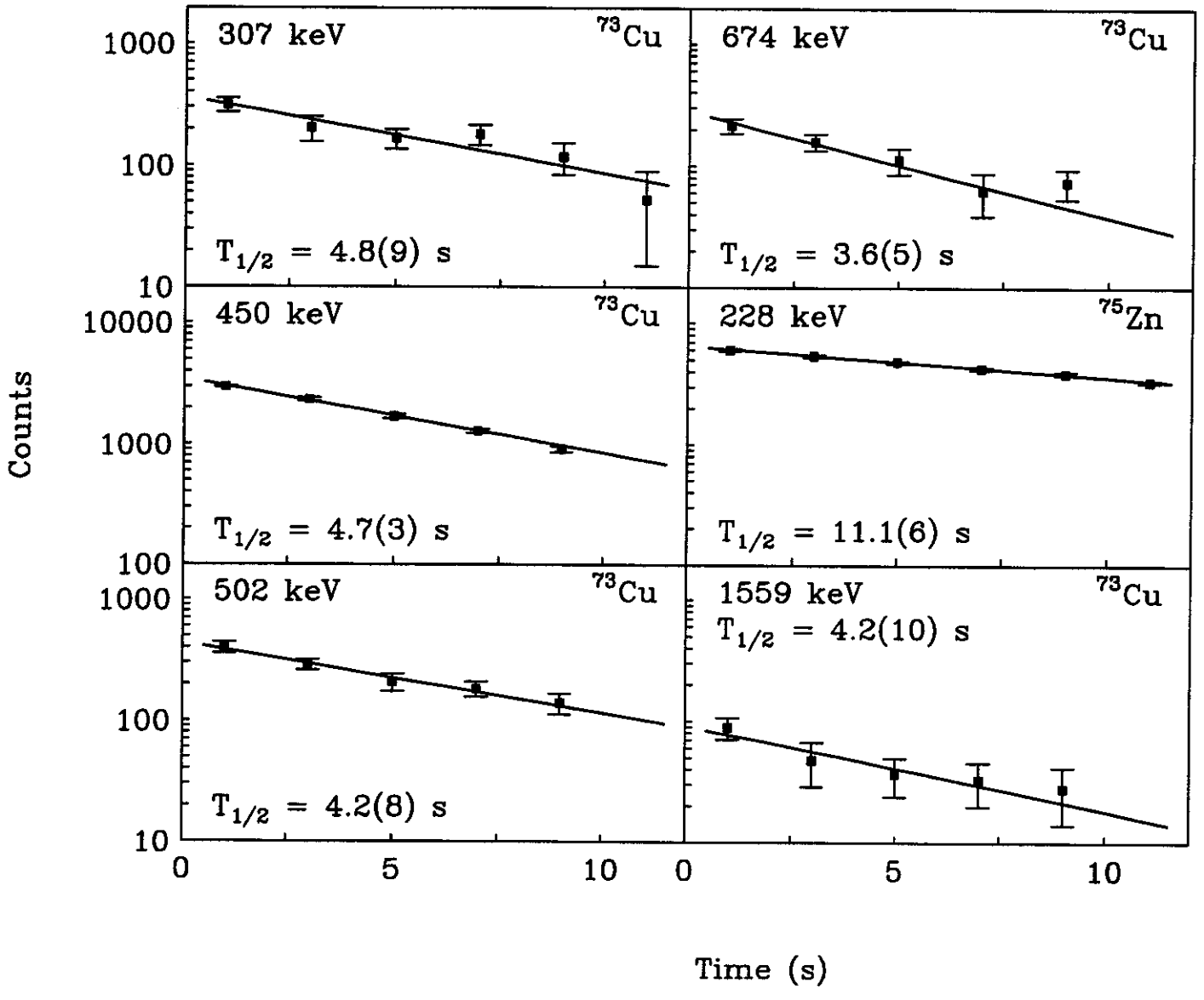
307 keV
^{73}Cu
$T_{1/2}$ = 4.8(9) s
674 keV
^{73}Cu
$T_{1/2}$ = 3.6(5) s
450 keV
^{73}Cu
$T_{1/2}$ = 4.7(3) s
228 keV
^{75}Zn
$T_{1/2}$ = 11.1(6) s
502 keV
^{73}Cu
$T_{1/2}$ = 4.2(8) s
1559 keV
^{73}Cu
$T_{1/2}$ = 4.2(10) s
Counts
Time (s)

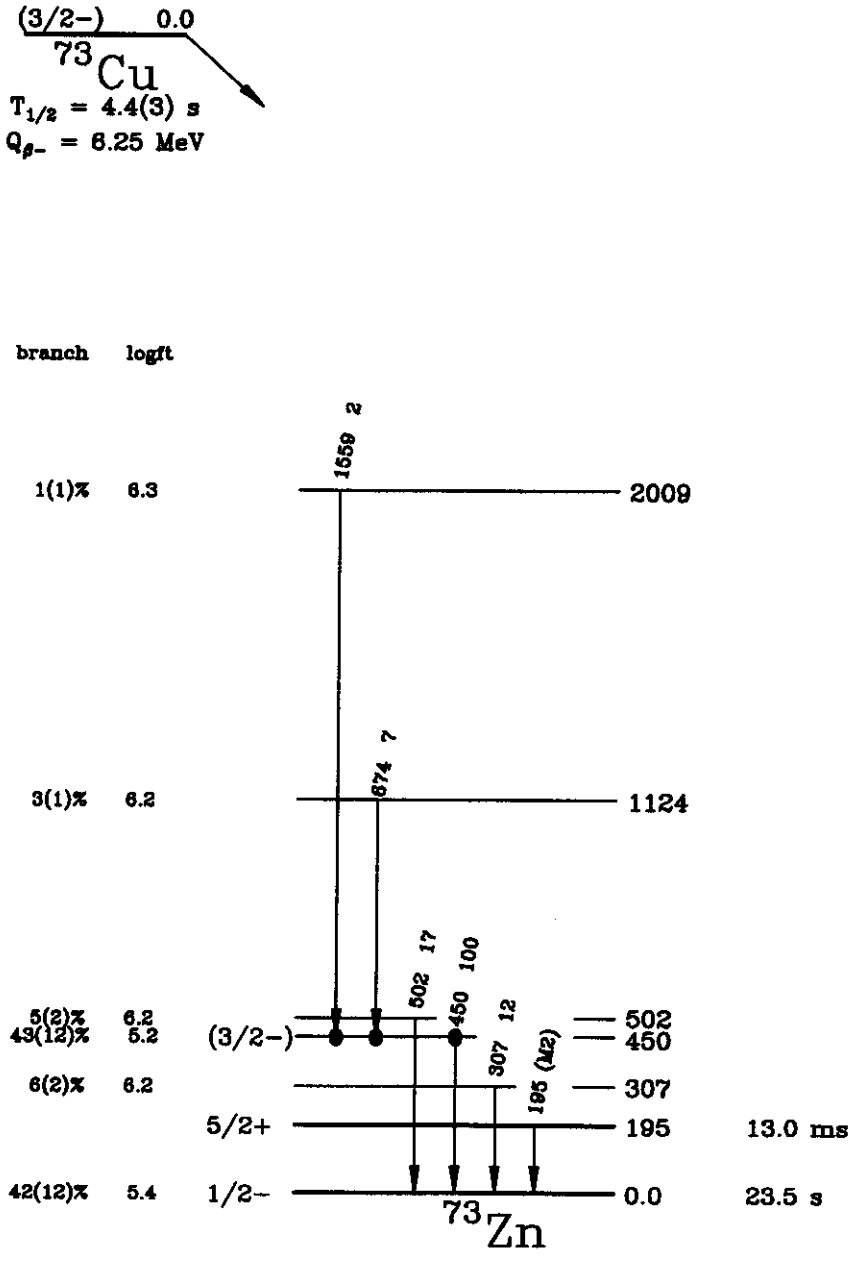
(3/2−) 0.0
73Cu
T1/2 = 4.4(3) s
Qβ− = 6.25 MeV
branch
logft
1(1)%
6.3
1559 2
2009
3(1)%
6.2
874 7
1124
5(2)%
6.2
43(12)%
5.2
(3/2−)
502 17
450 100
307 12
195 (M2)
502
450
307
6(2)%
6.2
5/2+
195
13.0 ms
42(12)%
5.4
1/2−
0.0
23.5 s
73Zn

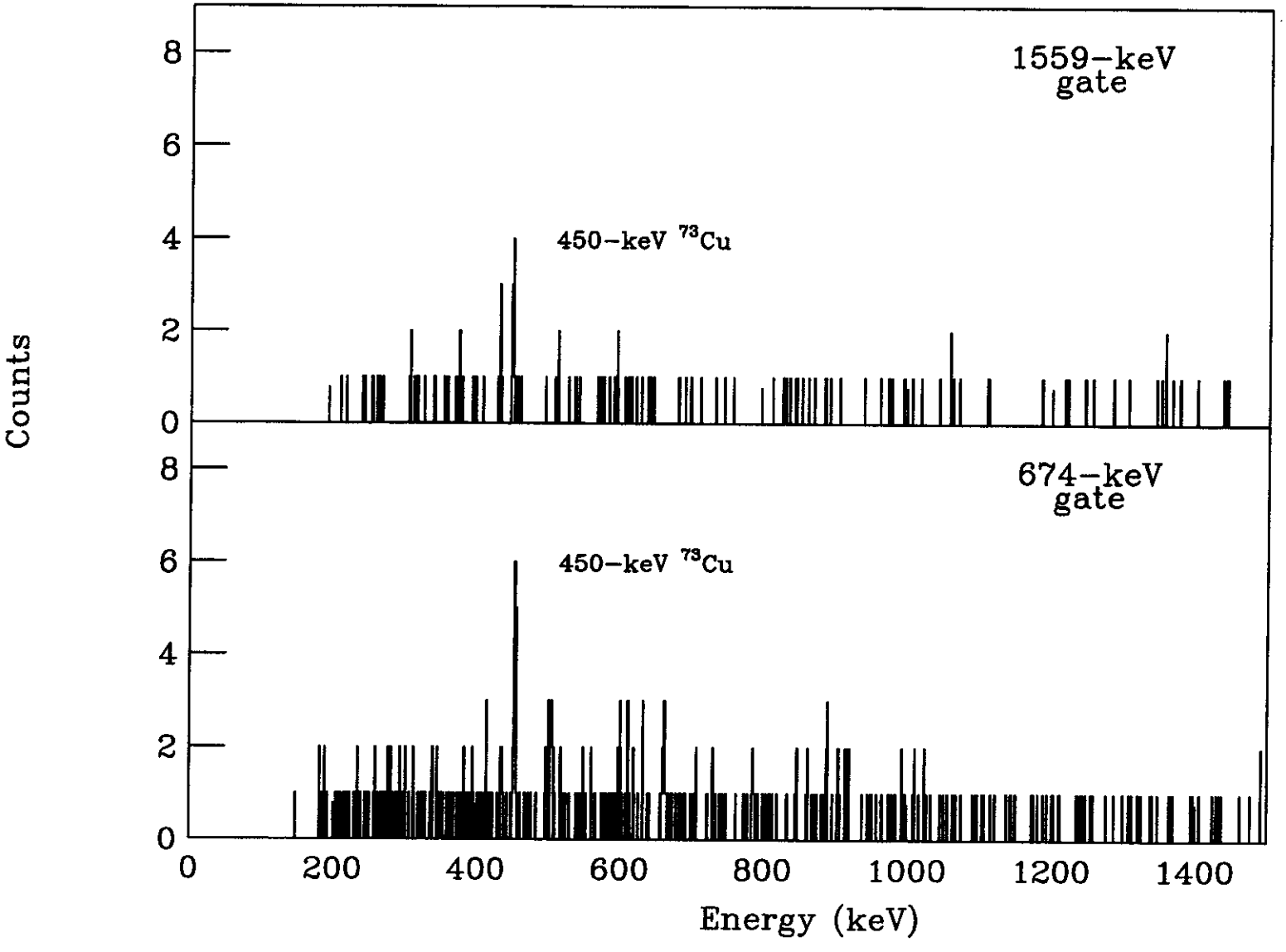
1559-keV
gate
450-keV ^{73}Cu
674-keV
gate
450-keV ^{73}Cu
Counts
Energy (keV)
0
2
4
6
8
0
200
400
600
800
1000
1200
1400

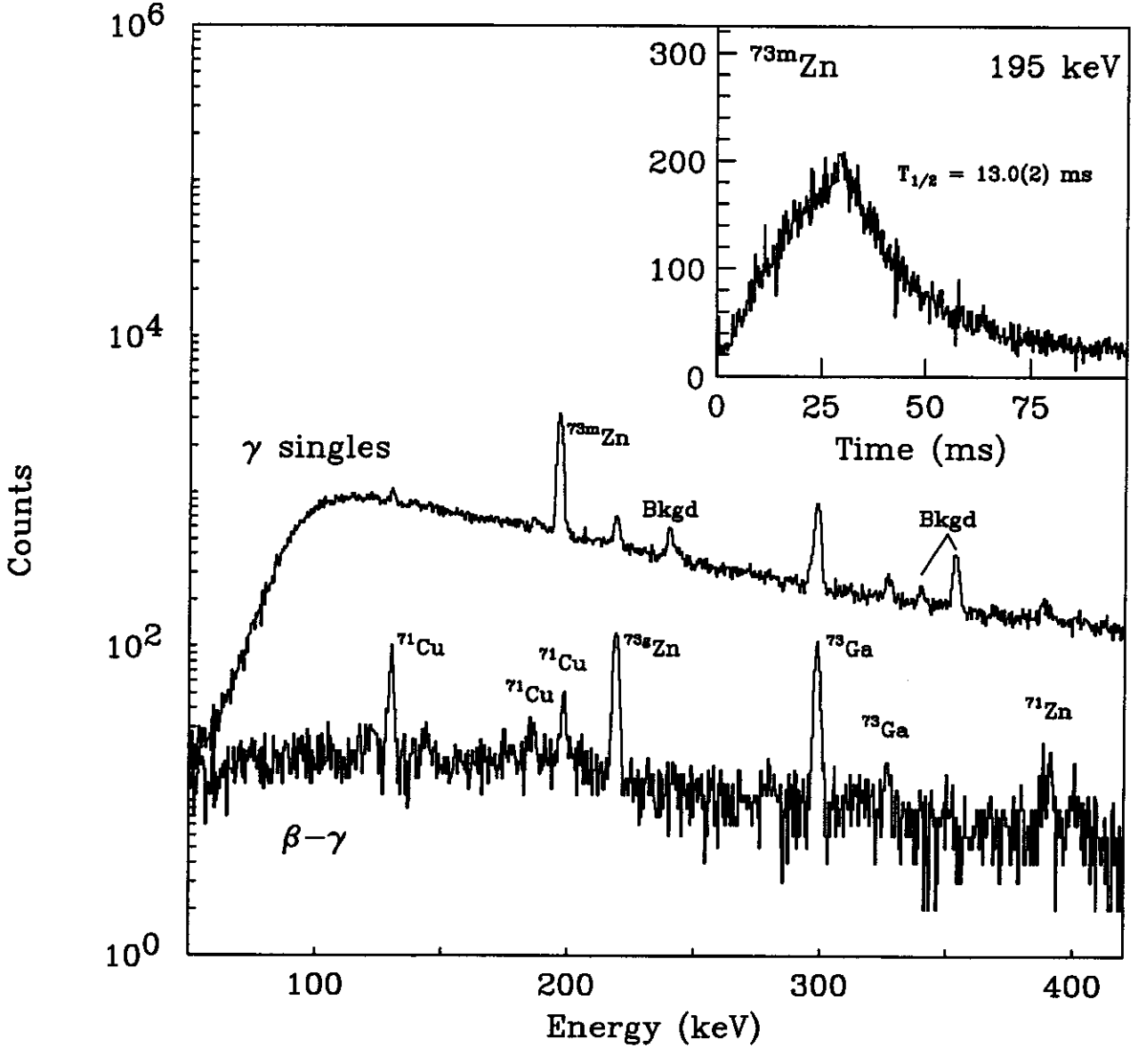
Counts
10^6
10^4
10^2
10^0
100
200
300
400
Energy (keV)
γ singles
$\beta-\gamma$
^{73m}Zn
Bkgd
Bkgd
^{71}Cu
^{71}Cu
^{71}Cu
^{73g}Zn
^{73}Ga
^{73}Ga
^{71}Zn
^{73m}Zn 195 keV
$T_{1/2}$ = 13.0(2) ms
300
200
100
0
0
25
50
75
Time (ms)

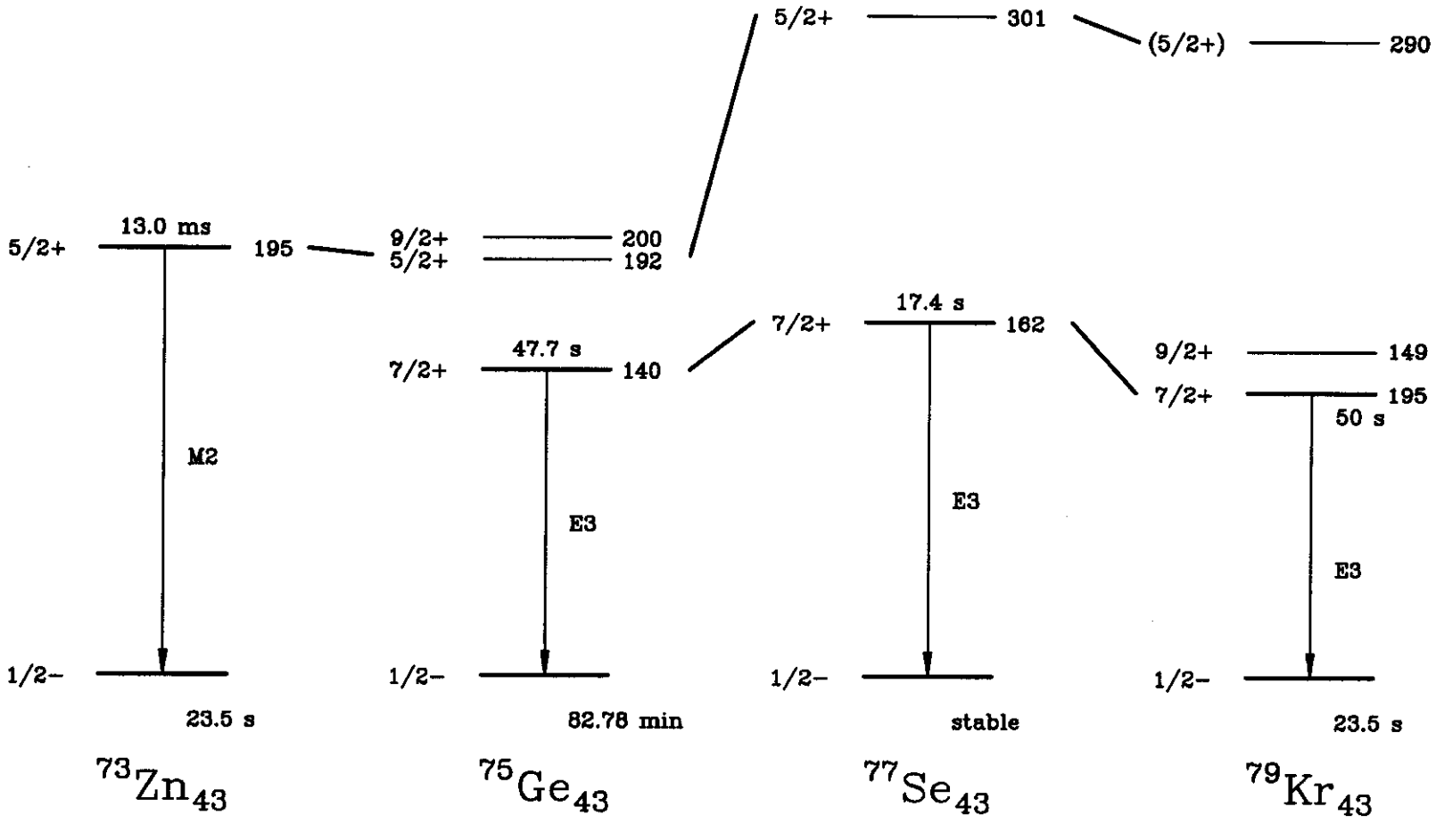
5/2+
13.0 ms
M2
1/2−
23.5 s
$^{73}Zn_{43}$
195
9/2+
200
5/2+
192
47.7 s
7/2+
140
E3
1/2−
82.78 min
$^{75}Ge_{43}$
5/2+
301
7/2+
17.4 s
162
E3
1/2−
stable
$^{77}Se_{43}$
(5/2+)
290
9/2+
149
7/2+
195
50 s
E3
1/2−
23.5 s
$^{79}Kr_{43}$

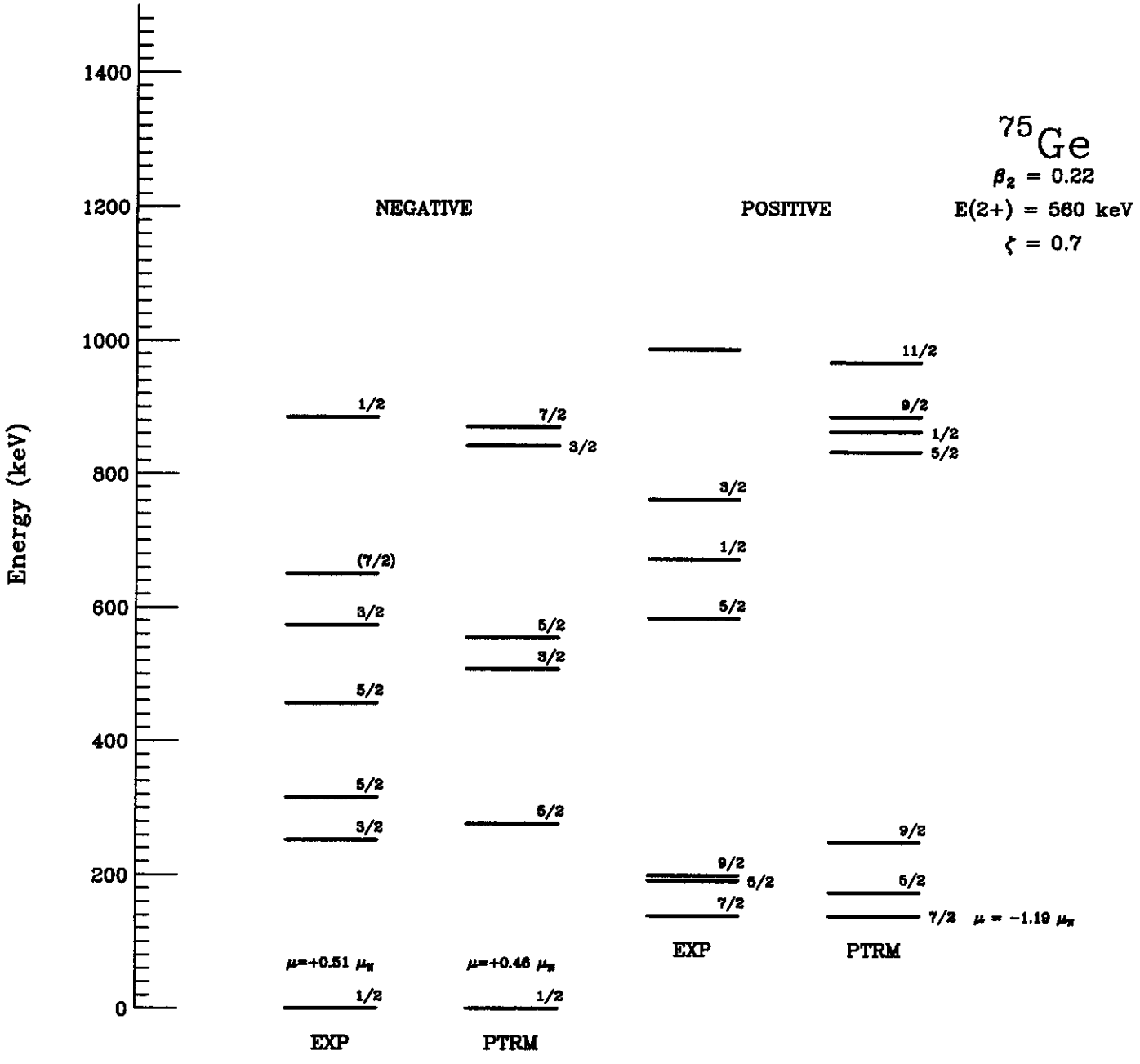
^{75}Ge
β_2 = 0.22
E(2+) = 560 keV
ζ = 0.7
NEGATIVE
POSITIVE
Energy (keV)
1400
1200
1000
800
600
400
200
0
1/2
(7/2)
3/2
5/2
5/2
3/2
μ=+0.51 μ_N
1/2
EXP
7/2
3/2
5/2
3/2
5/2
μ=+0.46 μ_N
1/2
PTRM
3/2
1/2
5/2
9/2
5/2
7/2
EXP
11/2
9/2
1/2
5/2
9/2
5/2
7/2 μ = −1.19 μ_N
PTRM

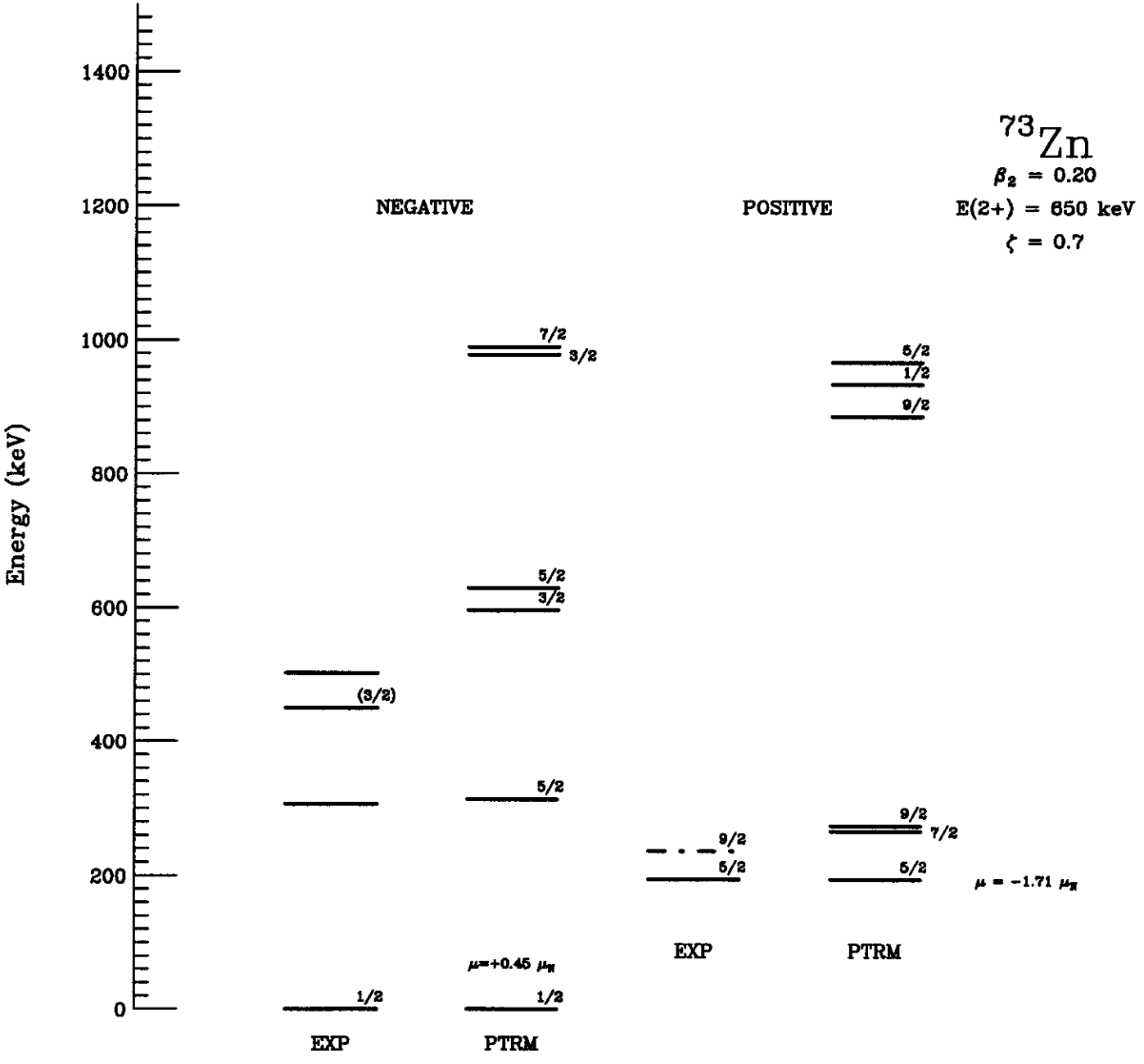
^{73}Zn
β_2 = 0.20
E(2+) = 650 keV
ζ = 0.7
NEGATIVE
POSITIVE
Energy (keV)
1400
1200
1000
800
600
400
200
0
7/2
3/2
5/2
3/2
5/2
(3/2)
1/2
1/2
μ=+0.45 μ_N
EXP
PTRM
9/2
5/2
EXP
9/2
7/2
5/2
PTRM
μ = −1.71 μ_N

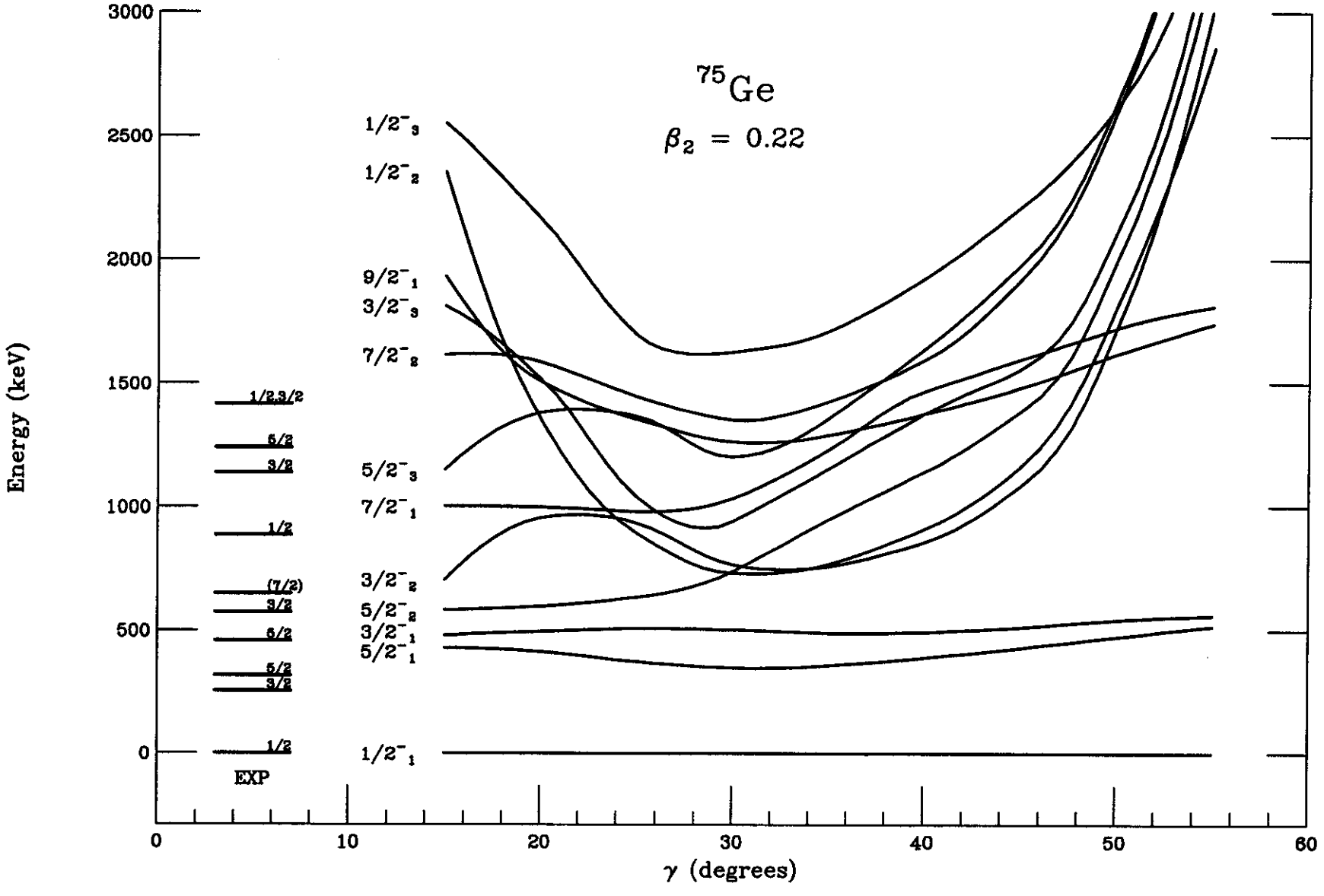
^{75}Ge
β_2 = 0.22
Energy (keV)
3000
2500
2000
1500
1000
500
0
1/2,3/2
5/2
3/2
1/2
(7/2)
3/2
5/2
5/2
3/2
1/2
EXP
$1/2^-_3$
$1/2^-_2$
$9/2^-_1$
$3/2^-_3$
$7/2^-_2$
$5/2^-_3$
$7/2^-_1$
$3/2^-_2$
$5/2^-_2$
$3/2^-_1$
$5/2^-_1$
$1/2^-_1$
0
10
20
30
40
50
60
γ (degrees)